ACS central science

Research Article

http://pubs.acs.org/journal/acscii

Tuning the Ground State Symmetry of Acetylenyl Radicals

Tao Zeng,[†] David Danovich,[‡] Sason Shaik,[‡] Nandini Ananth,[†] and Roald Hoffmann*[,†]

[†]Department of Chemistry and Chemical Biology, Cornell University, Ithaca, New York 14853, United States

[‡]Institute of Chemistry and The Lise Meitner-Minerva Center for Computational Quantum Chemistry, Hebrew University of Jerusalem, 91904 Jerusalem, Israel

Supporting Information

ABSTRACT: The lowest excited state of the acetylenyl radical, HCC, is a $^2\Pi$ state, only 0.46 eV above the ground state, $^2\Sigma^+$. The promotion of an electron from a π bond pair to a singly occupied σ hybrid orbital is all that is involved, and so we set out to tune those orbital energies, and with them the relative energetics of $^2\Pi$ and $^2\Sigma^+$ states. A strategy of varying ligand electronegativity, employed in a previous study on substituted carbynes, RC, was useful, but proved more difficult to apply for substituted acetylenyl radicals, RCC. However, π-donor/acceptor substitution is effective in modifying the state energies. We are able to design molecules with $^2\Pi$ ground states (NaOCC, H_2NCC ($^2A''$), HCSi, FCSi, etc.) and vary the $^2\Sigma^+$–$^2\Pi$ energy gap over a 4 eV range. We find an inconsistency between bond order and bond dissociation energy measures of the bond strength in the Si-containing molecules; we provide an explanation through an analysis of the relevant potential energy curves.

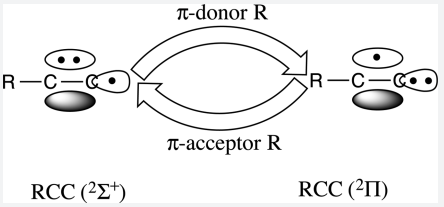

INTRODUCTION

The CH bond in acetylene is quite strong, 5.72 eV.[1,2] Homolytic CH cleavage leads to the acetylenyl radical HCC, a molecule that is a key intermediate in acetylene combustion[3,4] and has also been observed in a cold matrix,[5−7] in molecular beams,[8−10] and in the interstellar medium.[11−14] In astrochemistry and astrophysics, HCC serves as a detective species for carbon-rich environments.[15] It has also been proposed to be an intermediate in the formation of longer carbon chains,[16,17] larger unsaturated hydrocarbons, and carbon clusters[18] in space. The radical/H exchange reactions between HCC and unsaturated hydrocarbons are thought to play a role in astrochemistry and may be involved in the origin of life.[13,19−21] Similar reactions also lead to the formation of polycyclic aromatic hydrocarbons,[22] which in combustion environments eventually form soot.[23,24] HCC is thus an undesired species in combustion engineering.

Since a σ bond is broken in acetylene in forming HCC, a σ radical would be expected. And the ground state of HCC is indeed $^2\Sigma^+$. The surprise lies in the unexpectedly low energy of the first excited state of the radical, the $^2\Pi$ state—the experimental 0-0 transition energy is about 0.46 eV (3692 cm^{-1}).[25]

In a previous study, three of us (T.Z., N.A., and R.H.) saw our way to tune the difference between the doublet ($^2\Pi$) and quartet ($^4\Sigma^-$) states of carbynes, RC (or silylynes, RSi) over an astounding range, of more than 5 eV.[26] The configurations involved in these two spectroscopic states are shown in **1** and **2** in Scheme 1, with the σ orbital lying lower than the π orbital (−9.4 vs −1.7 eV of HC[27]).

The $^2\Pi$ and $^4\Sigma^-$ HC states differ in both spin multiplicity and spatial symmetry, whereas in HCC it is only a matter of spatial symmetry. Yet in both molecules the difference is in electronic occupations of σ vs π orbitals, as Figure 1 shows. The nonbonding π orbitals of CH, pure C $2p_x$ and $2p_y$, are transformed by bonding with another C in HCC into a lower π and an upper π^* combination.

Scheme 1. Electron Occupation Scheme of the $^2\Pi$ (1) and $^4\Sigma^-$ (2) States of Carbynes

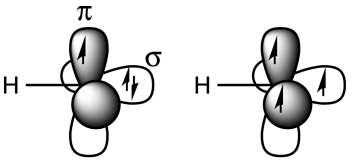

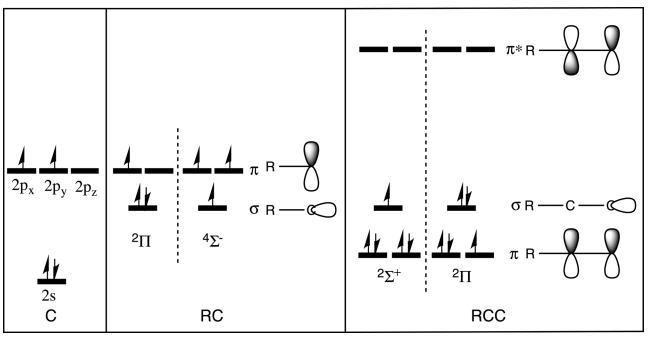

Figure 1. The rough positions and occupations of free carbon atom (left), RC (middle, both $^2\Pi$ and $^4\Sigma^-$ states), and RCC (right, both $^2\Sigma^+$ and $^2\Pi$ states) valence orbitals are indicated.

Received: May 8, 2015
Published: August 11, 2015

DOI: 10.1021/acscentsci.5b00187
ACS Cent. Sci. 2015, 1, 270−278

The $^2\Sigma^+$ ground state of HCC is well-described by the configuration $\pi^4\sigma^1$, the $^2\Pi$ excited state by $\pi^3\sigma^2$. Can we find an R that would invert the state order found in HCC? Could we tune the $^2\Sigma^+ - {}^2\Pi$ energy difference as dramatically as we did in HC? What might be the effect of changing either of the two C atoms for another group 14 element? The first objective of our study is to answer those questions. The computational methodology we use is specified in the Theoretical Methods section at the end of the paper.

An interesting species whose electronic states are related to those of HCC is its "deprotonated" anionic analogue C_2^-. It also has the same frontier orbital level ordering as HCC, with one interesting distinction. In C_2^- one also has σ_g above π_u, i.e., a $^2\Sigma_g^+$ ground state, with a short CC distance of 1.268 Å, and a $^2\Pi_u$ as the first doublet excited state, at a longer CC separation, 1.313 Å.[28,29] The difference between C_2^- and HCC is that the H−C bonding orbital (not shown in Figure 1) of the latter evolves into a relatively high-lying σ_u orbital of the former. The σ_u orbital of C_2^- has nonbonding character and higher energy, closer to the aforementioned π_u and σ_g orbitals. This makes the $B^2\Sigma_u^+$ excited state of C_2^-, which involves σ_u-to-σ_g excitation, lie only 2 eV above the ground state,[29,30] while the corresponding $X^2\Sigma^+$-to-$B^2\Sigma^+$ transition of HCC requires about 7 eV.[31]

The choice between the $^2\Sigma^+$ and $^2\Pi$ ground states of RCC is clearly related to tuning the σ and π orbital energies in the molecule: the higher the σ and lower the π orbital energy, the more likely is a $^2\Sigma^+$ ground state. The other way around favors a $^2\Pi$ ground state. Our experience with RC and RSi should guide us, but as we will see, there are important differences.

As mentioned above, HCC is an important interstellar species. Possessing a nonzero electric dipole moment, it can be observed through rotational transitions in its microwave spectrum.[11,15,32] These transitions display fine and hyperfine splittings due to spin-rotation coupling, electronic-nuclear spin coupling, spin−orbit coupling (SOC), and Λ-doubling (LD).[11,33−35] The projection of the electronic spatial angular momentum onto the molecular axis (0 for Σ and ±1 for Π) determines the presence of first-order SOC and LD in a specific electronic state (Σ, No; Π, Yes). As more and more elements heavier than H and He (known generally as "metals" in astronomy[36]) and functional groups are detected in the space,[37−41] we have reason to explore substituents other than H. Understanding the relation between the ligand R and the ground state symmetry of the molecule can facilitate identifications of RCC species based on the magnitude of the SOC- or LD-induced splitting, in interstellar space as well as combustion environments. This serves as a second motivation of the present work, in addition to our quest for further understanding of interesting radicals like RC, RCC, and C_2.

CONTRASTING HC AND HCC

The σ and π orbital energies in RCC can, in principle, be manipulated by changing σ/π donor/acceptor characteristics of R. HCC serves as our point of reference—a σ-donor, R, in RCC, is an element or group less electronegative than H, while a σ-acceptor involves a substituent more electronegative than H. A π-acceptor would be an R group with low-lying empty orbitals of π symmetry, capable of interacting with the π orbitals of the CC triple bond, such as CN, NO, NO_2, BR_2. And a π donor would be a substituent with high-lying filled π orbitals—NH_2, OH, a halogen.

It will be more difficult to change the ground state symmetry from $^2\Sigma^+$ to $^2\Pi$ than it was to effect an analogous $^2\Pi$ to $^4\Sigma^-$ change in RC. The reasons are as follows:

(1) In RCC the σ orbital has less density on R than in RC. This is qualitatively shown in Figure 2, one contour of the σ

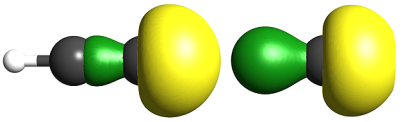

Figure 2. The σ Orbitals of HCC and HC (isosurfaces with value 0.1 au).

orbitals of HCC (left) and HC (right) taken from the $^2\Sigma^+$ and $^4\Sigma^-$ states, respectively. In those states, both σ orbitals are singly occupied (see Figure 1). More quantitatively, a Mulliken population analysis shows that the H contribution to the σ orbital of HCC is only 0.005, compared against 0.070 for the HC σ orbital. We hence expect that the RCC σ orbital will respond less to electronegativity change in R.

(2) The π orbitals in RC, pure 2p orbitals on C, are nonbonding, while those in RCC are CC bonding orbitals. The lack of bonding stabilization makes the π orbitals in RC more susceptible to π-acceptor manipulation. Energy arguments suggest greater sensitivity to π-donor substitution in RCC. But a second factor (affecting both π-donors and acceptors) enters: the acetylenyl π-system is spread out over two carbons, while that of RC is just on a single C. The Hamiltonian coupling matrix element in the interaction will be diminished in RCC for both acceptor and donor type perturbation.

This can be seen by the π orbital energies in the RC and RCC with R = H, CF_3 (a good π-acceptor), and NaO (a good π-donor). The energies are −1.7, −2.9, and 3.4 eV in HC, F_3CC, and NaOC, and −10.0, −11.0, and −5.6 eV in HCC, F_3CCC, and NaOCC.[42] Replacing H by a π-acceptor CF_3 (π-donor ONa), the π orbital energy is decreased (increased) noticeably more in RC than in RCC.

(3) An effect that we did not anticipate, but calculations show, is that the character (σ/π-donor/acceptor) of R is consistently blurred in RCC, and it is not straightforward to associate orbital energy variations with the character of R. This blurring is the result of commensurate first-order effects on the σ, and second-order effects on the π orbitals. This finding is not as mysterious as it sounds and is best illustrated through the examples below.

CASE STUDIES OF MODIFYING THE SUBSTITUENT R

We start with HCC. For this molecule, $^2\Sigma^+$ is the ground state, and $^2\Pi$ lies 0.51 eV higher (calculated, minimum-to-minimum). This energy interval compares favorably with the experimental value of 3692 cm^{-1} (0.46 eV) for the 0-to-0 excitation energy.[25] Both states are linear; the calculated and experimental bond lengths are given in Table 1. The satisfactory agreement in both molecular structure and excitation energy supports the accuracy of our methodology.

The $^2\Pi$ CC bond length is 0.08 Å longer than in the $^2\Sigma^+$ state. This is expected; the $\pi^3\sigma^2$ occupation of the $^2\Pi$ state generates a formal CC bond order of 2.5. The σ and π orbital energies are −9.7 and −10.0 eV. These two orbital energies will be taken as references in the discussion below. All calculated results reported here are at the level of General Multi-

DOI: 10.1021/acscentsci.5b00187
ACS Cent. Sci. 2015, 1, 270−278

Table 1. Calculated and Experimental Bond Lengths of the $^2\Sigma^+$ and $^2\Pi$ States of HCC[a]

	$^2\Sigma^+$		$^2\Pi$	
	calc.	exp.	calc.	exp.
r_{CH}/Å	1.056	1.050	1.062	1.060
r_{CC}/Å	1.211	1.210	1.288	1.289

[a]The experimental values are taken from ref 43. Note that we are qualitatively comparing calculated r_e and experimental r_0 values in this table.

Configurational Perturbation Theory (GMCPT) with properly chosen active spaces (see Theoretical Methods for details), unless further specified.

We begin the analysis of substituents with NaCC.[44] With such a strong σ-donor, we expect a flow of electrons into the σ system of the CC unit, raising the σ orbital energy. This is true; the σ energy is raised from −9.7 to −7.1 eV. We further expect the $^2\Sigma^+$ state to remain as the ground state, but with a larger excitation energy to the $^2\Pi$ state than in HCC. However, the π orbital energy is also raised, substantially so, from −10.0 to −7.0 eV. This is a second-order effect, albeit a large one. The negative charging of the CC piece of the molecule, by electron transfer in the σ system from Na to CC, raises the energy of the π orbitals (the π^* level is also raised from 7.7 to 9.7 eV). The net result is that the $^2\Pi$ lies only 0.37 eV higher than the $^2\Sigma^+$ state in our calculations.

Next we investigate a σ-acceptor, i.e., an electronegative substituent, in ClCC.[45] We find a $^2\Sigma^+$ ground state, with the $^2\Pi$ now lying only 0.11 eV higher. The two states are almost degenerate. The π energy remains invariant (−10.0 eV), and the σ orbital energy is decreased from −9.7 to −10.0 eV. Here the withdrawal of electron from the CC unit, a consequence of the greater electronegativity of Cl, makes the CC unit positive and lowers the σ orbital energy. The 0.3 eV decrease of the $\pi-\sigma$ orbital energy gap is commensurate with the 0.4 eV reduction of the $^2\Sigma^+-^2\Pi$ gap. It is worth mentioning that ClCC here (and $[ArCC]^+$ later) is a model system, and we do not consider the possibility of a bent structure, which is the case for FCC.[46]

The dilemma facing us emerges. The σ-electronegativity of the substituent R has little effect on the $\pi-\sigma$ orbital energy gap, mostly because of the small (e.g., from HCC to ClCC) and parallel (e.g., from HCC to NaCC) change in π and σ energies. This is in strong contrast to our findings for RC, where electronegativity affects the σ orbital energy more. We examine this difference in greater detail.

RC VS RCC

A comparison of electronegativity effects in RC (large) and RCC (small) is important at this point. In Figure 3, we summarize the change of orbital energies of RC and RCC with three representative ligands, electronegative Cl, "electronegativity-neutral" H, and electropositive Na. The trend in both RC and RCC is that as the electronegativity decreases (from Cl, to H, and to Na), both σ and π orbital energies are increased. One exception is that the π orbital energy decreases slightly by −0.1 eV from ClC to HC, a likely consequence of losing the π-donor effect of Cl, an effect separate from the electronegativity change. The difference between the upper and the lower halves of the figure is evident: unlike the almost parallel change in σ and π orbital energies of RCC from R = Cl to Na, the increase in σ orbital energy is more significant in RC.

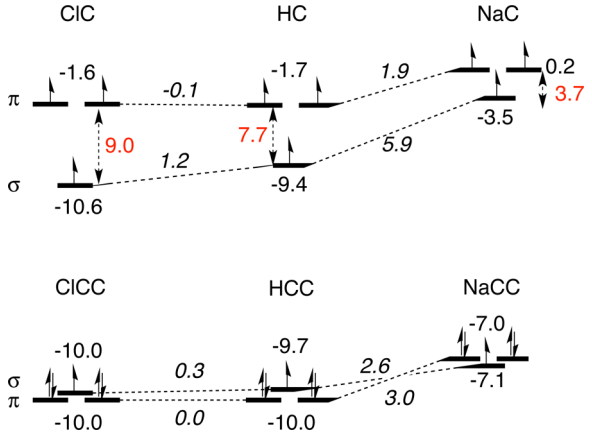

Figure 3. The energy positions of highest-lying occupied σ and π orbitals of RC and RCC with three representative ligands, Cl, H, and Na. The numbers by the orbital levels are their energies, those beside the connecting dashed lines (in italics) are the differential energies between the two connected levels, and those beside the vertical dashed double-headed arrows (in red) are the differential energies between the σ and π orbitals within the species. All numbers are in the unit of eV. For the lower half, the σ and π orbitals are close to each other, and their differential energies are not shown.

The different responses of the RC and RCC σ orbitals to the electronegativity of R have been analyzed thoroughly in the previous section. Note the evolution of the RCC σ, moving upward with decreasing electronegativity of R. The contribution that R makes, small as it is (Figure 2), to the σ orbital is responsible for this upward change.

For the π orbitals, their energy responses to the electronegativity change are not so different in RC and RCC, e.g., an increase of 1.9 eV from HC to NaC vs 2.6 eV from HCC to NaCC. The reason for the parallel behavior is that the electronegativity of R has similar consequences for the partial charge of the C in RC and that of the CC unit of RCC—the carbon segments of the molecules become negatively charged as the R electronegativity decreases, and the π orbital energies of RC and RCC thus rise. The parallel change of σ and π orbital energies of RCC with respect to the R electronegativity is supported by examining the energy changes from ClCC to $[ArCC]^+$. The more electronegative Ar^+ drags down the σ and π orbital energies from −10.0 to −16.4 and −17.5 eV, respectively, largely parallel decreases (−6.4 eV and −7.5 eV). Accompanying the decrease of σ and π orbital energies in $[ArCC]^+$ is a slight increase in $^2\Sigma^+-^2\Pi$ gap from 0.11 to 0.78 eV, consistent with the larger $\pi-\sigma$ energy gap (1.1 vs 0.0 eV).

The parallel change of σ and π orbital energies in the lower half of Figure 3 is indicative of the problem facing us: we cannot systematically tune the $^2\Sigma^+-^2\Pi$ energy order of RCC through changing the electronegativity of R. This is a situation very different from RC. Rather, we need to modify the π-donor/acceptor character of R, despite the predicted small response of π orbital energy in RCC compared with that in RC.

π-EFFECTS

We examined a series of R substituents with different π-donor/acceptor character; the differential energies between the $^2\Pi$ and $^2\Sigma^+$ states of those RCC are shown in Table 2, along with the σ and π orbital energies and their differences. $\Delta_{\Pi-\Sigma}$ indicates the energy difference between the two terms: $E(^2\Pi) - E(^2\Sigma^+)$, positive for $^2\Sigma^+$ state lower, negative for $^2\Pi$ state lower. Some

DOI: 10.1021/acscentsci.5b00187
ACS Cent. Sci. 2015, 1, 270−278

Table 2. Differential Energies between $^2\Pi$ and $^2\Sigma^+$ ($\Delta_{\Pi-\Sigma} = E(^2\Pi) - E(^2\Sigma^+)$), σ and π Orbital Energies (E_σ and E_π), Differential Energies between the Two Orbitals ($\Delta_{\sigma-\pi} = E_\sigma - E_\pi$), the Symmetry of the Optimized Structures, and the Term Symbols in the Structures That Correlate to the $^2\Pi$ and $^2\Sigma^+$ Terms in Linear Structure[a]

species	$\Delta_{\Pi-\Sigma}$	E_σ	E_π	$\Delta_{\sigma-\pi}$	symmetry and terms[b]
$[NCC]^{2-}$	−2.81	3.8	7.1	−3.3	linear
$[HNCC]^-$	−1.87	−3.1	−0.8	−2.3	C_s, $^2\Sigma^+$ to $^2A'$, $^2\Pi$ to $^2A''$
$[OCC]^-$	−1.40	−2.9	−0.9	−2.0	linear
NaOCC	−0.82	−7.1	−5.6	−1.5	linear
H_2NCC	−0.61	−9.2	−7.8	−1.4	C_s, $^2\Sigma^+$ to $^2A'$, C_{2v}, $^2\Pi$ to $^2A''$[c]
HSCC	−0.23	−9.9	−8.8	−1.1	C_s, $^2\Sigma^+$ to $^2A'$, $^2\Pi$ to $^2A''$
HOCC	−0.21	−9.7	−8.6	−1.1	C_s, $^2\Sigma^+$ to $^2A'$, $^2\Pi$ to $^2A''$
NCCC	0.33	−10.8	−10.4	−0.4	linear
HCC	0.51	−9.7	−10.0	0.3	linear
OBCC	0.62	−10.7	−11.0	0.3	linear
F_3CCC	0.66	−10.6	−11.0	0.4	C_{3v}, $^2\Sigma^+$ to $^2A_1$, C_s, $^2\Pi$ to $^2A''$[d]
$[OCCC]^+$	1.12	−17.2	−18.2	1.0	linear

[a]All energies are in the unit of eV. [b]Coordinates of all species are given in the Supporting Information. [c]For H_2NCC, the $^2\Sigma^+$ term has a C_s structure, and the $^2\Pi$ has a C_{2v} structure. [d]For F_3CCC, the $^2\Sigma^+$ term has a C_{3v} structure, and the $^2\Pi$ has a C_s structure.

of the RCC species have nonlinear structures, and the term symbols $^2\Pi$ and $^2\Sigma^+$ are then applied only approximately to them. The actual term symbols to which the $^2\Pi$ and $^2\Sigma^+$ correlate are also shown in the table, with the symmetry of the species being specified. For C_s molecules, the doubly degenerate $^2\Pi$ term splits into two, $^2A'$ and $^2A''$. We consider here only the ones with lower energy; they all turn out to be $^2A''$.

The molecules in Table 2 are sorted in order of increasing $^2\Pi-^2\Sigma^+$ differential energies. The order roughly follows the π-donor/π-acceptor character of the ligands. The molecules with a $^2\Pi$ ($^2\Sigma^+$) ground state have a π-donor (acceptor) ligand.

The π-effects are readily demonstrated by the $\sigma-\pi$ orbital energy gap. A π-donor ligand generally gives a small, negative orbital energy gap (σ below π, reverse in the order shown in Figure 1), while a π-acceptor gives a large, positive orbital gap. The correlation between the $^2\Pi-^2\Sigma^+$ energy gaps (selection of ground state symmetry) and the $\sigma-\pi$ orbital energy gaps (π-effects) in Table 2 is clearly seen in Figure 4, with the red plus markers. The fitted trend line also shown in Figure 4 has a slope close to 1, reflecting the orbital gap's determining influence on the state gap. Our strategy of using π-effects to tune the ground state symmetry of RCC works — a 4 eV range in term splitting is pretty good.

EXTENDING THE CARBON CHAIN

Another systematic way to reverse the $\sigma-\pi$ and $^2\Pi-^2\Sigma^+$ energy orders is worth mentioning. If one were to extend the carbon chain by two carbons, or four, the particle-in-box nature of the oligoacetylenoid π orbitals tells us that for each C≡C unit added to the chain, the energy of the highest occupied π orbital rises, as an extra node is introduced. This is so even as the highest occupied and lowest unoccupied π orbitals do not converge to the same energy, a consequence of bond

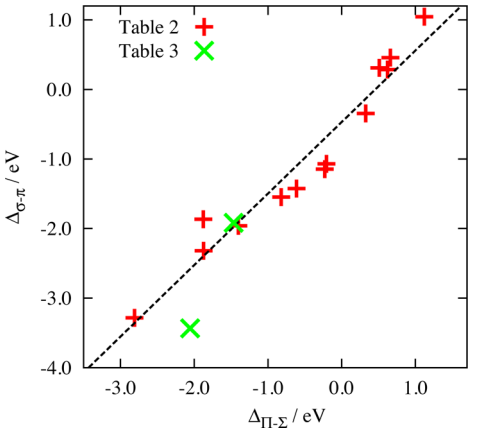

Figure 4. Correlation between the state and orbital energy gaps in Table 2 (red plus) and Table 3 (green cross). The trend line is fitted to the Table 2 data, with the equation $y = 1.0283x - 0.4693$ and the coefficient of determination $R^2 = 0.94$.

alternation. Figure 5a shows the highest occupied π orbitals explicitly for HCC, HC_4, and HC_6. Meanwhile, the σ orbital energy remains largely invariant as the added C≡C unit is "electronegativity-neutral" with respect to the original C≡C fragment.

The different responses of the σ and π orbitals will ultimately make the π orbital higher than the σ. The argument is not original to us, as Figure 5b, reproduced from the work of Pauzat and Ellinger[47] shows. At the level of Hückel theory, this crossover was found to occur at HC_6. This reverse in orbital energy order leads to the fact that HCC and HC_4 have a $^2\Sigma^+$ ground state,[48,49] while HC_6 and those longer have a $^2\Pi$ ground state.[50,51] Near the crossover, one encounters some very small state differences, which in turn lead to an excellent laboratory for studying the Renner−Teller effect. The molecules in question, HC_n, n = 1−12, are of prime interest to the astrophysical community, as they have been observed in the interstellar medium.[52] We have confirmed the computational results cited for the doublet states of HC_4.

REPLACING ONE C BY SI

Our success in tuning the ground state symmetry of RCC through modification of the π orbital energy encourages us to move to a stronger perturbation, replacing one of the C atoms by Si. Si is known to have less propensity to form a good π bond.[53] The substitution will then raise the energy of the π orbital and localize it at the C site, while decreasing the energy of the π^* orbital and localizing it at the Si. The substitution can thus reverse the $\sigma-\pi$ orbital energy gap and favor a $^2\Pi$ ground state.

Table 3 shows the $^2\Pi-^2\Sigma^+$ gaps for HCSi and FCSi. For both cases, the $^2\Pi$ state is now the ground state. Si-substitution gives an exceptionally strong preference for the $^2\Pi$ ground state, such that the $^2\Pi$ state lies as much as 1.47 and 2.05 eV lower than the $^2\Sigma^+$ state! Only some negatively charged RCC species in Table 2 have such low-lying $^2\Pi$ states. We also investigated the other Si-substituted molecules, HSiC and FSiC. Although they both have $^2\Pi$ ground state at their linear structure, they are subject to a significant Renner−Teller effect[54] and distort to bent structures, whose ground states cannot be clearly associated with $^2\Pi$ or $^2\Sigma^+$.

Plotted in Figure 6a is the π orbital of HCSi. As expected, the orbital is localized on the C site, and its energy (listed in Table

DOI: 10.1021/acscentsci.5b00187
ACS Cent. Sci. 2015, 1, 270−278

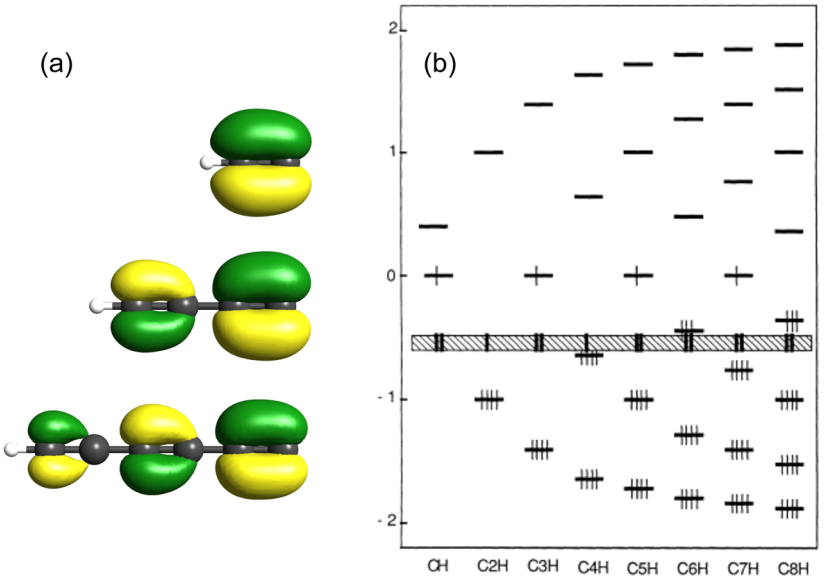

Figure 5. (a) CASSCF calculated highest occupied π orbitals of HCC, HC_4, and HC_6 (isosurfaces with value 0.1 au); (b) Hückel energy diagram in units of -β for the π and top σ orbitals in the HC_n series. The striped area gives the approximate position of the σ orbitals. Panel (b) is a reproduction of Figure 1 in Pauzat, F. and Ellinger, Y. *Astron. Astrophys.* Vol. 216, pp 305−309, 1989 (Ref. 47), reproduced with permission ©ESO. Here one only needs to focus on the HC_n chains with an even number of carbon atoms.

Table 3. Differential Energies (eV) between $^2\Pi$ and $^2\Sigma^+$ States ($\Delta_{\Pi-\Sigma} = E(^2\Pi) - E(^2\Sigma^+)$), σ and π Orbital Energies (E_σ and E_π), Differential Energies between the Two Orbitals ($\Delta_{\sigma-\pi} = E_\sigma - E_\pi$), and Electric Dipole Moment of the Two States (μ_Π and μ_Σ) of the Two RCSi Molecules[a]

species	$\Delta_{\Pi-\Sigma}$[b]	E_σ	E_π	$\Delta_{\sigma-\pi}$	μ_Π; μ_Σ[c]
HCSi	−1.47	−9.1	−7.2	−1.9	0.48; −1.43
FCSi	−2.05	−10.6	−7.1	−3.5	−0.37; −2.34

[a]All energies are in the unit of eV. Dipole moments are in the unit of Debye. [b]GMCPT/cc-pVTZ. [c]Positive dipole moment here indicates that the Si end carries a negative partial charge, while the H or F end is positive. The dipole moments are obtained using CASSCF wave functions in GMCPT calculations. The more advanced Multi-Reference Configuration Interaction (MRCI) method with a full valence active space gives the same trend of dipole moment change: 0.31 and −1.50 D for HCSi; −0.03 and −2.15 D for FCSi.

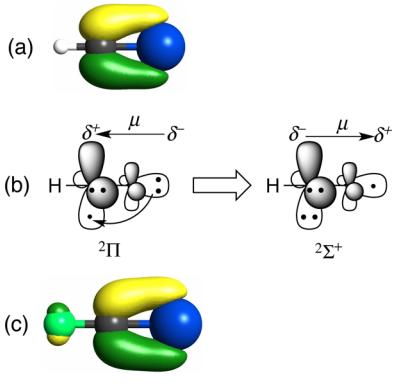

Figure 6. (a) π bonding orbitals of HCSi, (b) schematic electron rearrangement involved in the $^2\Pi$-to-$^2\Sigma^+$ transition in HCSi, and (c) Si−C π bonding orbitals with antibonding contribution from F in FCSi. The isosurfaces in (a) and (c) correspond to the value 0.1 au. In (b) the solid arrows with "μ" on top indicate the direction of the dipole moment, with the δ^+ and δ^- at the two ends indicating the partial charge.

3) is substantially higher than that of HCC, −7.1 vs −10.0 eV. In addition to the weaker C−Si π bonding mentioned in the beginning of this section, cramming most of the π electrons onto the C site also contributes to this increase in energy. The variation of the σ orbital energy is small, from −9.7 eV of HCC to −9.1 eV of HCSi. The σ hybrid on Si should have been significantly higher in energy than that on C due to the different electronegativities of the two elements. The reason for this mild 0.6 eV increase in energy is that the positive charge on Si mitigates the energy rise. Overall, the $\sigma-\pi$ energy gap is reversed from 0.3 eV of HCC to −1.9 eV of HCSi, resulting in a $^2\Pi$ ground state.

While the negative $\sigma-\pi$ energy gap is largely responsible for the $^2\Pi$ state being lower than the $^2\Sigma^+$ state, the gap between those two states is further enhanced by the charge-transfer character of the excitation. As shown in Figure 6b, the $^2\Pi$-to-$^2\Sigma^+$ transition of HSiC involves moving an electron from the Si-localized σ lone pair to the C-localized π bonding orbital. Transferring one more electron to the already electron-rich C and creating a hole in the already electron-deficient Si require a higher energy, resulting in the large state gap.

The charge transfer picture also explains the sign change in electric dipole moment accompanying the $^2\Pi$-to-$^2\Sigma^+$ transition of HCSi. The state-specific dipole moments are listed in Table 3. The $^2\Pi$ ground state features an outward-protruding σ hybrid orbital that contributes substantially, in a manner leading to a "positive" dipole moment, i.e., pointing from the terminal Si to the H. In determining the dipole moment direction, the σ lone pair outcompetes the reverse polarization of the electrons in the σ_{C-Si} and π_{C-Si} bonding orbitals, arising from the electronegativity difference between C and Si. The result is a small positive dipole (0.48 D); the situation is similar to the famous anomalous dipole direction of CO.[55] However, in the interatomic transition from Si to C shown in Figure 6b, the balance between the electronegativity (pro-negative dipole) and the σ hybrid (pro-positive dipole) effects is broken, and the dipole moment flips from 0.48 to −1.43 D.

DOI: 10.1021/acscentsci.5b00187
ACS Cent. Sci. 2015, 1, 270−278

With the antibonding interaction to the π orbital induced by substituting H by F, shown in Figure 6c, the $\sigma-\pi$ gap is increased in magnitude from −1.9 eV in HCSi to −3.5 eV in FCSi. The magnitude of the $^2\Pi-^2\Sigma^+$ gap is correspondingly increased from 1.47 to 2.05 eV, resulting in the "most favored" $^2\Pi$ ground state of all neutral species investigated in this work. The charge transfer argument above for HCSi is also applicable for FCSi; the magnitude of electric dipole moment is reduced from −2.34 to −0.37 D during the $^2\Pi$-to-$^2\Sigma^+$ transition. But this time, the electronegative F outcompetes the charge-transfer excitation in determining the dipole direction, and the dipole flip does not occur.

The state gaps and orbital gaps of HCSi and FCSi are also plotted in Figure 4. As expected, they do not fall on the trend line for the RCC data, but the general correlation is maintained.

HOW CAN A SEEMINGLY MORE WEAKLY BONDED STATE BECOME THE GROUND STATE?

Scheme 2 shows Lewis dot structures for the two states of HCSi. On the basis of their MO occupation schemes, the $^2\Sigma^+$ state may be described by a C−Si triple bond and an odd electron in the σ nonbonding orbital. The $^2\Pi$ state has a C−Si bond order of 2.5 since one of the π bonds contains only a single electron.

Scheme 2. Comparison of Lewis Structures, C−Si Bond Lengths (R_e), Bond Dissociation Energies (D_e), and Force Constants (k) of the $^2\Sigma^+$ and $^2\Pi$ States of HCSi

$^2\Sigma^+$	$^2\Pi$
H−C≡Si (•)	H−C≐Si (••)
R_e = 1.607 Å	R_e = 1.690 Å
D_e = 4.26 eV	D_e = 5.57 eV
k = 7.4 N/cm	k = 5.5 N/cm

Scheme 2 also compares bond lengths (R_e), bond dissociation energies (D_e, without zero point energy correction), and harmonic force constants (k) of the two states. The formally stronger triple bond of the $^2\Sigma^+$ state is shorter, as expected, and the R_e and k are correlated qualitatively according to the Badger's Rule,[56,57] i.e., a shorter bond has a larger k. Nevertheless, a seeming inconsistency rises up when one judges the bond strengths using D_e. The $^2\Pi$ state with a formally lower bond order has a larger D_e — it is harder, energetically, to break the C−Si bond in this state. A study of FCSi reveals a similar inconsistency, but here our discussion is focused on the representative HCSi. The two D_e's in Scheme 2 are calculated using the same ground state dissociation limit of HC ($^2\Pi$) and Si (^3P_g). Note that the difference between the two D_e's is 1.31 eV, noticeably different from the 1.47 eV $\Delta_{\Pi-\Sigma}$ reported in Table 3. This is because the D_e's are obtained in a state-averaged fashion, while the state energies in Table 3 are obtained through state-specific calculations. This quantitative difference does not affect our discussion.

To gain insight into the apparent contradiction between the short (long) bond length and low (high) D_e of the relevant states, we calculate the potential energy curves (PECs) of the lowest-lying $^2\Pi$ and $^2\Sigma^+$ states, *two of each*, of HCSi along the C−Si distance. Roman numbers I and II are used to distinguish states of the same symmetry, with State I having lower energy. The H−C distance is kept fixed at the ground state bond length, 1.070 Å. The PECs are shown in Figure 7. In accordance with Scheme 2, we find the $^2\Sigma^+$(I) state to have a minimum at a shorter C−Si distance, and we observe a sharper well around the minimum than the $^2\Pi$(I) state. While the $^2\Sigma^+$(I) PEC rises steeply to a high energy dissociation limit, which should have given it a large D_e, it encounters the PEC of $^2\Sigma^+$(II) and undergoes an avoided crossing at the C−Si distance around 2.7 Å. The $^2\Sigma^+$(I) gains repulsive character in this avoided crossing and its PEC slopes down to the ground state dissociation limit of HC ($^2\Pi$) and Si (^3P_g).

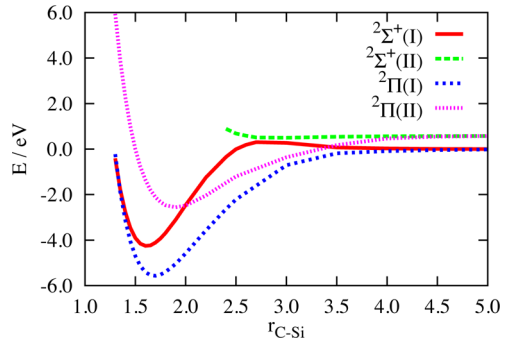

Figure 7. Adiabatic potential energy curves of the lowest two $^2\Sigma^+$ and two $^2\Pi$ states of HCSi as functions of C−Si distance. We only show the green curve at r_{C-Si} > 2.3 Å since it represents a $^2\Delta$ state (due to the $^2\Delta-^2\Sigma^+$ crossing and both Δ and Σ^+ correlate to the A_1 irreducible representation of C_{2v}, the highest Abelian subgroup of $C_{\infty v}$ that we actually used in our calculation) at the shorter distance. This segmented $^2\Sigma^+$(II) PEC does not affect our understanding of the avoided crossing between the two $^2\Sigma^+$ states.

We can now reconcile the inconsistency between the $^2\Sigma^+$ state's short bond and low D_e: the dissociation limit that is used to calculate its D_e does not match well the character of the state near its equilibrium separation. The relatively small D_e of 4.26 eV is not reflective of the underlying bond strength of the $^2\Sigma^+$ state. A similar avoided crossing argument was used to account for the mismatch between the D_e and k of the C_2 molecule. However, the avoided crossing in the C_2 case is quite large and reduces the corresponding force constant, not only the dissociation energy.[58]

The ground $^2\Pi$ state of HCSi also undergoes an avoided crossing, at about r_{C-Si} = 3.0 Å (Figure 7). But it is a mitigated one, in comparison to the $^2\Sigma^+$ avoided crossing, and there is no "bend-down" of its PEC. The 5.57 eV D_e hence represents the bond strength of the $^2\Pi$ state more appropriately.

We conclude that bond length and force constant are more indicative of what qualitatively is taken to be the "bond strength". Dissociation energies require a careful analysis of dissociation limit states and intervening level crossings.[2] The literature contains examples of a variety of bonds where the bond length, force constants, and the dissociation energies are in "mismatch"; a particularly clear exposition for Sn−Sn bonds has been given by Kaupp and co-workers.[59] Those cases may constitute genuine breakdowns of the Badger rule.

OTHER STRATEGIES

In addition to the strategies introduced here, there may be yet other approaches to tune the ground state symmetry of RCC. One way is to directly modify the σ orbital energy by attaching a σ-acceptor (acid (A), such as BH_3). The resultant RCCA molecule will have a $^2\Pi$ ground state, but it should not be considered as an RCC radical.

DOI: 10.1021/acscentsci.5b00187
ACS Cent. Sci. 2015, 1, 270−278

Another option is through hydrogen bonding. Placing a hydrogen bond donor (HF, say) near the terminal C of RCC and pointing its H toward the σ hybrid may induce one electron to transfer from the fully occupied π to the singly occupied σ orbital, forming a σ lone pair while maintaining the chemical identity of RCC. However, due to the strong C−H bond of acetylene, it is very likely that the RCC will abstract an H atom from the hydrogen-bond provider. For instance, the O−H bond of H_2O is weaker than the C−H bond of acetylene (5.15[60] vs 5.72 eV of bond dissociation energy), and H-abstraction occurs readily.[61] With a stronger bond (5.91 eV[60] dissociation energy), HF may be a better candidate. Another challenge in this strategy is ensuring that the hydrogen bond donor adopts the right position and orientation. Considering this, HF is not a good candidate, as our optimized structure for the [HCC-HF] complex has the HF pointing toward the π orbital; i.e., the π bond pair donates electrons to form the hydrogen bond. Seeking an appropriate hydrogen bond donor to tune the RCC ground state symmetry is an interesting subject for future research.

CONCLUSIONS

From the outset we knew that it would be more difficult to manipulate the $^2\Sigma^+$−$^2\Pi$ energy order and spacing in RCC than in RC. This is because the σ orbital energy responds less dramatically to electronegativity change in R, an outcome of the localization of the σ hybrid and the subsequent small R contribution in it. Also, in a second-order effect, the π system of the CC part of the molecule is affected in a parallel way to the σ orbital by the electronegativity of R.

Nevertheless, we find it possible to tune the $^2\Sigma^+$−$^2\Pi$ energy order and spacing through π-donor/acceptor effects of the ligand R, as well as by substituting one of the two C atoms by Si. The acetylenyl π orbital energy can be increased, making it close in energy to the σ orbital of the molecule. And the overall $^2\Sigma^+$−$^2\Pi$ term energy difference can be made positive. In the end, the $^2\Sigma^+$−$^2\Pi$ gap can be tuned over a range of at least 4 eV, from negative to positive. The apparent inconsistency between the high bond order and low bond dissociation energy in the $^2\Sigma^+$ state of the molecules with a $^2\Pi$ ground state that we observe in the Si-substituted species is explained. The low bond dissociation energy stems from avoided crossing and does not reflect the bond strength.

The revealed relation between the character of the ligand R and the ground state symmetry of RCC will facilitate identification in future spectroscopic investigations of such molecular species in the interstellar medium and in combustion environments.

THEORETICAL METHODS

The GMCPT method[62−64] is used to optimize structure and calculate state energy for most of the molecules, except as further specified. This methodology accounts for both dynamical and nondynamical correlations of electrons. The active space is selected to include the C−C (or C−Si) π bonding, π^* antibonding, and the terminal σ orbitals, and all electrons distributed among them. When R is a π-donor, the two filled π orbitals on R are included in the active space. Similarly, when R is a π-acceptor, the low-lying empty π-orbitals of R are included. The active space of each molecule is given in the Supporting Information along with its geometry. The reported orbital energies come from the Complete Active Space Self-Consistent Field (CASSCF) step in the GMCPT calculations. The cc-pVTZ basis set is used throughout. GMCPT and CASSCF calculations were done with the GAMESS-US program package,[65,66] and MRCI with Molpro 2010.[67] All molecular structures are plotted using MacMolPlt 7.4.4.[68]

ASSOCIATED CONTENT

Supporting Information

The Supporting Information is available free of charge on the ACS Publications website at DOI: 10.1021/acscentsci.5b00187.

More avoided crossings of the $^2\Sigma^+$ states of HCSi; optimized coordinates, active spaces, and calculated energies of all RCC and RCSi species (PDF)

AUTHOR INFORMATION

Corresponding Author

*E-mail: rh34@cornell.edu.

Notes

The authors declare no competing financial interest.

ACKNOWLEDGMENTS

T.Z. gratefully acknowledges the Natural Sciences and Engineering Research Council of Canada for the Banting Postdoctoral Fellowship (201211BAF-303459-236530). R.H.'s thinking on the acetylenyl radical was stimulated by a correspondence with Ray Firestone. R.H. is grateful to the National Science Foundation for its support of this work through Grant CHE-1305872. S.S. acknowledges support by the Israel Science Foundation (Grant ISF 1183/13). N.A. acknowledges start-up funding from Cornell University.

REFERENCES

(1) Ervin, K. M.; Gronert, S.; Barlow, S. E.; Gilles, M. K.; Harrison, A. G.; Bierbaum, V. M.; Depuy, C. H.; Lineberger, W. C.; Ellison, G. B. Bond strengths of ethylene and acetylene. *J. Am. Chem. Soc.* **1990**, *112*, 5750−5759.

(2) Danovich, D.; Hiberty, P. C.; Wu, W.; Rzepa, H. S.; Shaik, S. The nature of the fourth bond in the ground state of C_2: The quadruple bond conundrum. *Chem. - Eur. J.* **2014**, *20*, 6220−6232.

(3) Williams, A.; Smith, D. B. Combustion and oxidation of acetylene. *Chem. Rev.* **1970**, *70*, 267−293.

(4) Nguyen, V. S.; Elsamra, R. M. I.; Peeters, J.; Carl, S. A.; Nguyen, M. T. Experimental and theoretical study of the reaction of the ethynyl radical with nitrous oxide, C_2H + N_2O. *Phys. Chem. Chem. Phys.* **2012**, *14*, 7456−7470.

(5) Jacox, M. E.; Olson, W. B. The $\tilde{A}^2\Pi$−$\tilde{X}$ $^2\Sigma^+$ transition of HC_2 isolated in solid argon. *J. Chem. Phys.* **1987**, *86*, 3134−3142.

(6) Shepherd, R. A.; Graham, W. R. M. FTIR study of D and ^{13}C substituted C_2H in solid argon. *J. Chem. Phys.* **1987**, *86*, 2600−2605.

(7) Forney, D.; Jacox, M. E.; Thompson, W. E. The infrared and near-infrared spectra of HCC and DCC trapped in solid neon. *J. Mol. Spectrosc.* **1995**, *170*, 178−214.

(8) Zhang, F.; Kim, S.; Kaiser, R. I. A crossed molecular beams study of the reaction of the ethynyl radical ($C_2H(X^2\Sigma^+)$) with allene ($H_2CCCH_2(X^1A_1)$). *Phys. Chem. Chem. Phys.* **2009**, *11*, 4707−4714.

(9) Blush, J. A.; Park, J.; Chen, P. A high-intensity molecular beam of vinyl and ethynyl radicals. *J. Am. Chem. Soc.* **1989**, *111*, 8951−8953.

(10) Jones, B.; Zhang, F.; Maksyutenko, P.; Mebel, A. M.; Kaiser, R. I. Crossed molecular beam study on the formation of phenylacetylene and its relevance to Titan's atmosphere. *J. Phys. Chem. A* **2010**, *114*, 5256−5262.

(11) Tucker, K. D.; Kutner, M. L.; Thaddeus, P. The ethynyl radical C_2H — a new interstellar molecule. *Astrophys. J.* **1974**, *193*, L115−L119.

DOI: 10.1021/acscentsci.5b00187
ACS Cent. Sci. 2015, 1, 270−278

(12) Beuther, H.; Semenov, D.; Henning, T.; Linz, H. Ethynyl (C_2H) in massive star formation: tracing the initial conditions? *Astrophys. J.* **2008**, *675*, L33−L36.
(13) Ziurys, L. M. The chemistry in circumstellar envelopes of evolved stars: Following the origin of the elements to the origin of life. *Proc. Natl. Acad. Sci. U. S. A.* **2006**, *103*, 12274−12279.
(14) Lucas, R.; Liszt, H. S. Comparative chemistry of diffuse clouds. I. C_2H and C_3H_2. *Astron. Astrophys.* **2000**, *358*, 1069−1076.
(15) Huggins, P. J.; Carlson, W. J.; Kinney, A. L. The distribution and abundance of interstellar C_2H. *Astron. Astrophys.* **1984**, *133*, 347−356.
(16) Goulay, F.; Soorkia, S.; Meloni, G.; Osborn, D. L.; Taatjes, C. A.; Leone, S. R. Detection of pentatetraene by reaction of the ethynyl radical (C_2H) with allene (CH_2═C═CH_2) at room temperature. *Phys. Chem. Chem. Phys.* **2011**, *13*, 20820−20827.
(17) Vuitton, V.; Scemama, A.; Gazeau, M.-C.; Chaquin, P.; Benilan, Y. IR and UV spectroscopic data for polyynes: Predictions for long carbon chain compounds in Titan's atmosphere. *Adv. Space Res.* **2001**, *27*, 283−288.
(18) Bettens, R. P. A.; Herbst, E. The formation of large hydrocarbons and carbon clusters in dense interstellar clouds. *Astrophys. J.* **1997**, *478*, 585−593.
(19) Kaiser, R. I. The role of cyano (CN) and ethynyl (C_2H) radicals in astrobiology and implications to the origin of life on earth. *Eur. Space Agency, Special Pub.* **2001**, *495*, 145−153.
(20) Kaiser, R. I.; Balucani, N. Astrobiology — the final frontier in chemical reaction dynamics. *Int. J. Astrobiol.* **2002**, *1*, 15−23.
(21) Kaiser, R. I.; Mebel, A. M. On the formation of polyacetylenes and cyanopolyacetylenes in titans atmosphere and their role in astrobiology. *Chem. Soc. Rev.* **2012**, *41*, 5490−5501.
(22) Ghesquière, P.; Talbi, D. On the formation of naphthalene cation in space from small hydrocarbon molecules: a theoretical study. *Chem. Phys. Lett.* **2013**, *564*, 11−15.
(23) Parker, D. S. N.; Mebel, A. M.; Kaiser, R. I. The role of isovalency in the reactions of the cyano (CN), boron monoxide (BO), silicon nitride (SiN), and ethynyl (C_2H) radicals with unsaturated hydrocarbons acetylene (C_2H_2) and ethylene (C_2H_4). *Chem. Soc. Rev.* **2014**, *43*, 2701−2713.
(24) Marsh, N. D.; Wornat, M. J. Formation pathways of ethynyl-substituted and cyclopenta-fused polycyclic aromatic hydrocarbons. *Proc. Combust. Inst.* **2000**, *28*, 2585−2592.
(25) Sharp-Williams, E. N.; Roberts, M. A.; Nesbitt, D. J. High resolution slit-jet infrared spectroscopy of ethynyl radical: $^2\Pi$−$^2\Sigma^+$ vibronic bands with sub-Doppler resolution. *J. Chem. Phys.* **2011**, *134*, 064314.
(26) Zeng, T.; Wang, H.; Lu, Y.; Xie, Y.; Wang, H.; Schaefer, H. F.; Ananth, N.; Hoffmann, R. Tuning spin-states of carbynes and silylynes: A long jump with one leg. *J. Am. Chem. Soc.* **2014**, *136*, 13388−13398.
(27) In this paper, we choose to report all RC orbital energies obtained in state-averaged CASSCF calculations, which weight equally the $^4\Sigma^-$ and $^2\Pi$ states ($^4\Sigma^-$: $^2\Pi_x$: $^2\Pi_x$ = 0.5:0.25:0.25) in Scheme 1, so that both occupation schemes are treated equally.
(28) Herzberg, G.; Lagerqvist, A. A new spectrum associated with diatomic carbon. *Can. J. Phys.* **1968**, *46*, 2363−2373.
(29) Mead, R. D.; Hefter, U.; Schulz, P. A.; Lineberger, W. C. Ultrahigh resolution spectroscopy of C_2^-: The $A^2\Pi_u$ state characterized by deperturbation methods. *J. Chem. Phys.* **1985**, *82*, 1723−1731.
(30) Nichols, J. A.; Simons, J. Theoretical study of C_2 and C_2^-: *X* $^1\Sigma^+_g$, *a* $^3\Pi_u$, *X* $^2\Sigma^+_g$, and *B* $^2\Sigma^+_u$ potentials. *J. Chem. Phys.* **1987**, *86*, 6972−6981.
(31) Fortenberry, R. C.; King, R. A.; Stanton, J. F.; Crawford, T. D. A benchmark study of the vertical electronic spectra of the linear chain radicals C_2H and C_4H. *J. Chem. Phys.* **2010**, *132*, 144303.
(32) Tucker, K. D.; Kutner, M. L. The abundance and distribution of interstellar C_2H. *Astrophys. J.* **1978**, *222*, 859−862.
(33) Sharp-Williams, E. N.; Roberts, M. A.; Nesbitt, D. J. High resolution slit-jet infrared spectroscopy of ethynyl radical: $^2\Pi$−$^2\Sigma^+$ vibronic bands with sub-Doppler resolution. *J. Chem. Phys.* **2011**, *134*, 064314.
(34) Tarroni, R.; Carter, S. Theoretical calculation of absorption intensities of C_2H and C_2D. *Mol. Phys.* **2004**, *102*, 2167−2179.
(35) Tarroni, R.; Carter, S. Theoretical calculation of vibronic levels of C_2H and C_2D to 10000 cm^{-1}. *J. Chem. Phys.* **2003**, *119*, 12878−12889.
(36) Ferrière, K. M. The interstellar environment of our galaxy. *Rev. Mod. Phys.* **2001**, *73*, 1031−1066.
(37) Barone, V.; Biczysko, M.; Puzzarini, C. Quantum chemistry meets spectroscopy for astrochemistry: Increasing complexity toward prebiotic molecules. *Acc. Chem. Res.* **2015**, *48*, 1413−1422.
(38) Herbst, E.; Yates, J. T. Introduction: astrochemistry. *Chem. Rev.* **2013**, *113*, 8707−8709.
(39) Herbst, E.; van Dishoeck, E. F. Complex organic interstellar molecules. *Annu. Rev. Astron. Astrophys.* **2009**, *47*, 427−480.
(40) Brown, W. A. Astrochemistry. *Phys. Chem. Chem. Phys.* **2014**, *16*, 3343−3343.
(41) Sakai, N.; Yamamoto, S. Warm carbon-chain chemistry. *Chem. Rev.* **2013**, *113*, 8981−9015.
(42) All orbital energies of RCC reported in this work are obtained from state-averaged CASSCF calculations that weight equally the $^2\Sigma^+$ and $^2\Pi$ states ($^2\Sigma^+$: $^2\Pi_x$: $^2\Pi_x$ = 0.5:0.25:0.25), so that both occupation schemes are treated equally.
(43) Kuchitsu, K., Ed. *Structure of Free Polyatomic Molecules — Basic Data*; Springer-Verlag: Berlin, 1998; p 123.
(44) We do not present LiCC here, so as to minimize the π-acceptance effects.
(45) We also calculated FCC, but the F π-donation obscures the effect we seek to understand.
(46) Tarroni, R.; Palmieri, P.; Rosmus, P. On the lowest electronic states of the C_2F radical. *Int. J. Quantum Chem.* **1996**, *60*, 467−473.
(47) Pauzat, F.; Ellinger, Y. The lowest two electronic states of the hexatriynil radical — C_6H. *Astron. Astrophys.* **1989**, *216*, 305−309.
(48) Mazzotti, F. J.; Raghunandan, R.; Esmail, A. M.; Tulej, M.; Maier, J. P. Characterization of C_4H in the $A^2\Pi$ and $X^2\Sigma^+$ states by double resonance four-wave mixing. *J. Chem. Phys.* **2011**, *134*, 164303.
(49) Yu, S.; Su, S.; Zhang, Y.; Dai, D.; Yuan, K.; Yang, X. Photodissociation dynamics of C_4H_2 at 164.41 nm: Competitive dissociation pathways. *J. Chem. Phys.* **2013**, *139*, 124307.
(50) Gottlieb, C. A.; McCarthy, M. C.; Thaddeus, P. Vibrationally excited C_6H. *Astrophys. J., Suppl. Ser.* **2010**, *189*, 261−269.
(51) Zhao, D.; Haddad, M. A.; Linnartz, H.; Ubachs, W. C_6H and C_6D: Electronic spectra and Renner-Teller analysis. *J. Chem. Phys.* **2011**, *135*, 044307.
(52) See the relevant entries in www.astro.uni-koeln.de/cdms/molecules.
(53) Jutzi, P. New element-carbon (p-p)π bonds. *Angew. Chem., Int. Ed. Engl.* **1975**, *14*, 232−245.
(54) Renner, R. Zur Theorie der Wechselwirkung zwischen Elektronen — und Kernbewegung bei dreiatomigen, stabförmigen Molekülen. *Eur. Phys. J. A* **1934**, *92*, 172−193.
(55) Scuseria, G. E.; Miller, M. D.; Jensen, F.; Geertsen, J. The dipole moment of carbon monoxide. *J. Chem. Phys.* **1991**, *94*, 6660−6663.
(56) Badger, R. M. A Relation Between Internuclear Distances and Bond Force Constants. *J. Chem. Phys.* **1934**, *2*, 128−131.
(57) Badger, R. M. The Relation Between the Internuclear Distances and Force Constants of Molecules and Its Application to Polyatomic Molecules. *J. Chem. Phys.* **1935**, *3*, 710−714.
(58) Shaik, S.; Danovich, D.; Wu, W.; Su, P.; Rzepa, H. S.; Hiberty, P. C. Quadruple bonding in C_2 and analogous eight-valence electron species. *Nat. Chem.* **2012**, *4*, 195−200.
(59) Kaupp, M.; Metz, B.; Stoll, H. Breakdown of bond length-bond strength correlation: a case study. *Angew. Chem., Int. Ed.* **2000**, *39*, 4607−4609. See also the references therein.
(60) Blanksby, S. J.; Ellison, G. B. Bond dissociation energies of organic molecules. *Acc. Chem. Res.* **2003**, *36*, 255−263.

DOI: 10.1021/acscentsci.5b00187
ACS Cent. Sci. 2015, 1, 270−278

(61) Ding, Y.-H.; Zhang, X.; Li, Z.-S.; Huang, X.-R.; Sun, C.-C. Is the C_2H+H_2O reaction anomalous? *J. Phys. Chem. A* **2001**, *105*, 8206−8215.
(62) Nakano, H.; Uchiyama, R.; Hirao, K. Quasi-degenerate perturbation theory with general multiconfiguration self-consistent field reference functions. *J. Comput. Chem.* **2002**, *23*, 1166−1175.
(63) Miyajima, M.; Watanabe, Y.; Nakano, H. Relativistic quasidegenerate perturbation theory with four-component general multiconfiguration reference functions. *J. Chem. Phys.* **2006**, *124*, 044101.
(64) Ebisuzaki, R.; Watanabe, Y.; Nakano, H. Efficient implementation of relativistic and non-relativistic quasidegenerate perturbation theory with general multiconfigurational reference functions. *Chem. Phys. Lett.* **2007**, *442*, 164−169.
(65) Schmidt, M. W.; Baldridge, K. K.; Boatz, J. A.; Elbert, S. T.; Gordon, M. S.; Jensen, J. H.; Koseki, S.; Matsunaga, N.; Nguyen, K. A.; Su, S.; Windus, T. L.; Dupuis, M.; Montgomery, J. A. General atomic and molecular electronic structure system. *J. Comput. Chem.* **1993**, *14*, 1347−1363.
(66) Gordon, M. S. and Schmidt, M. W. Advances in electronic structure theory: GAMESS a decade later. In *Theory and Applications of Computational Chemistry: The First Forty Years*; Dykstra, C. E., Frenking, G., Kim, K. S., Scuseria, G. E., Eds.; Elsevier: Amsterdam, 2005.
(67) Werner, H.-J., Knowles, P. J., Manby, F. R., Schütz, M. and et al. *MOLPRO*, version 2010.1, a package of ab initio programs; see http://www.molpro.net.
(68) Bode, B. M.; Gordon, M. S. MacMolPlt: a graphical user interface for GAMESS. *J. Mol. Graphics Modell.* **1998**, *16*, 133−138.

DOI: 10.1021/acscentsci.5b00187
ACS Cent. Sci. 2015, 1, 270−278